Learning Science Through Research
Published by the Keck Geology Consortium
Short Contributions
Keck Geology Consortium
Volume 37
May 2025
doi: 10.18277/AKRSG.2025.37.01

TESTING MODELS OF NORMAL FAULT SYSTEM EVOLUTION, DAMAGE ZONE DEVELOPMENT, AND GEOTHERMAL POTENTIAL

BENJAMIN SURPLESS, Trinity University

INTRODUCTION

Because seismic hazard assessment and natural resource development rely on prediction of fault behavior, structural geologists commonly model the evolution of fault systems to better understand their long-term evolution. Researchers have established that faults perturb local stress fields as they propagate, influencing the formation of minor faults and intense fracturing in an envelope, or "damage zone", around them (Fig. 1) (e.g., Peacock and Sanderson, 1996; Shipton and Cowie, 2003; Kim et al., 2004; Choi et al., 2016). These damage zones increase rock permeability, which enhances groundwater flow rates (e.g., Rowley, 1998), hydrocarbon migration (e.g., Morley et al., 1990), ore mineralization (e.g., DeWitt et al., 1986), and geothermal energy production potential (e.g., Siler et al., 2018; Shervais et al., 2024).

In addition, although researchers have long recognized that fault zones are segmented, as opposed to continuous, planar surfaces (e.g., Tchalenko, 1970; Schwartz and Coppersmith, 1984), researchers have made significant advances in the role that segmentation plays in overall fault system evolution (e.g., Long and Imber, 2011; Siler et al., 2018; Surpless and Thorne, 2021) as well as how interacting faults affect damage zone development (e.g., Kim et al., 2004; Choi et al., 2016). Where two adjacent normal fault segments interact, fracturing is commonly amplified, increasing the volume of rock damaged relative to two separate, isolated faults (e.g., Stock and Hodges, 1990; Hudson, 1992; Faulds, 1996).

Recent studies suggest that damage zones may not develop symmetrically on either side of a fault plane; instead, damage zone development may be asymmetric, with one side (hanging wall or footwall) displaying a greater thickness than the other (e.g., Berg and Skar, 2005; Ferrill et al., 2011; Liao et al., 2020). In addition, researchers debate whether the

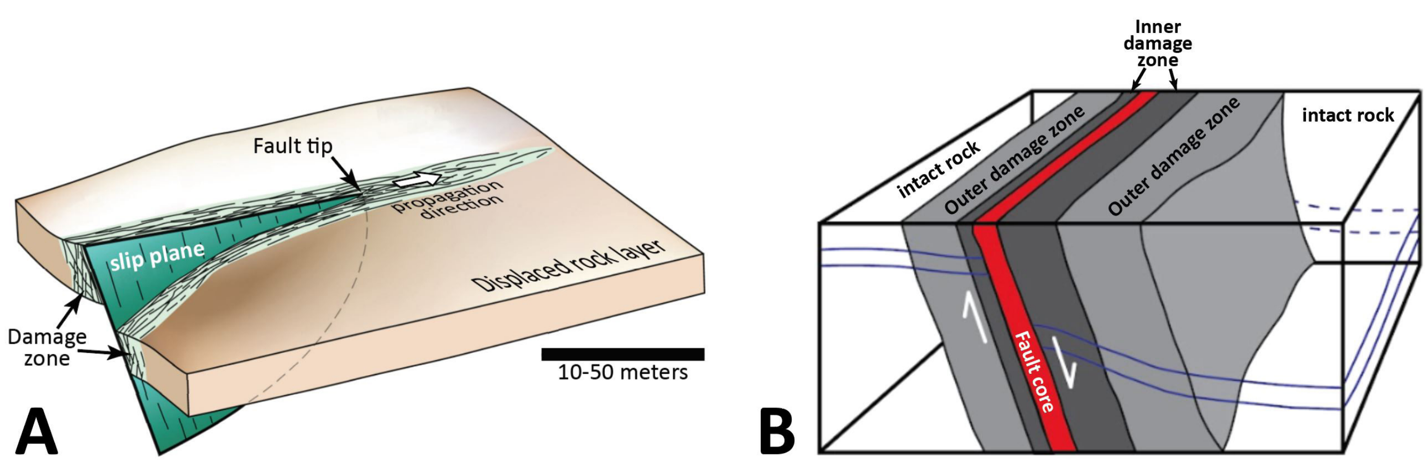

Figure 1. Development of a fault damage zone during normal fault propagation and displacement. A. damage zone development ahead of a propagating, elliptical fault tip and parallel to the fault plane (adapted from Fossen, 2016). B. Damage zone architecture and terminology (adapted from Laio et al., 2020).

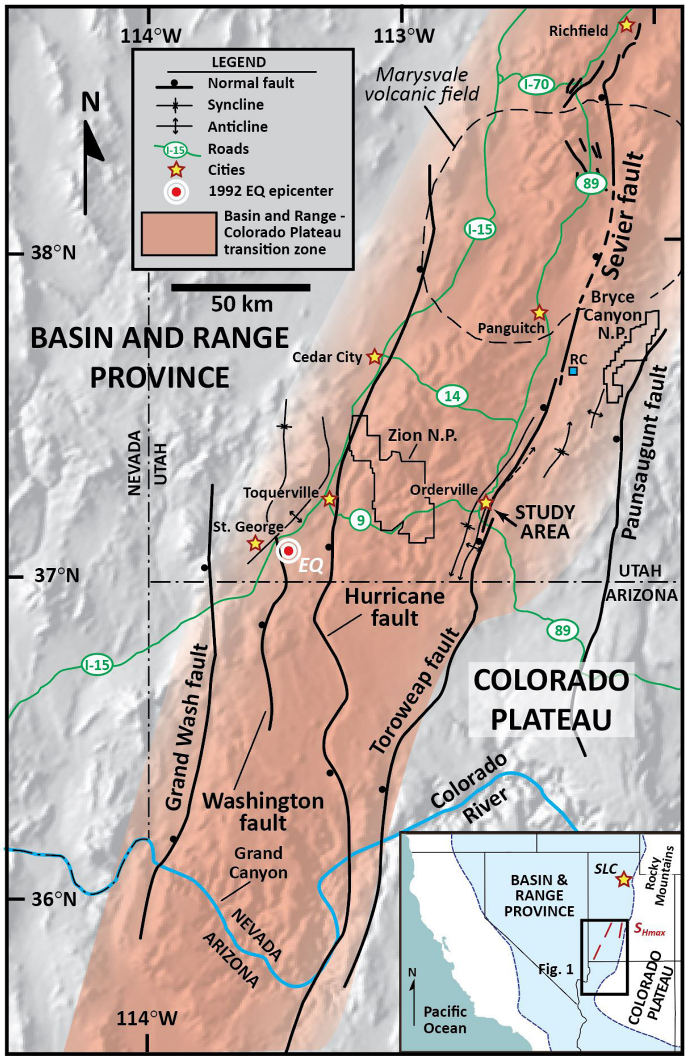

Figure 2. The Sevier fault zone study area within the Basin and Range-Colorado Plateau transition zone [see inset, with the location of Salt Lake City (SLC) indicated with a star]. The red lines on the inset figure are orientations of the maximum horizontal stress field (SHmax) as constrained by Lundstern and Zoback (2020). The Sevier-Toroweap fault, the Grand Wash fault, the Washington fault, the Hurricane fault, and the Paunsaugunt fault accommodate extension across the transition zone. Ball is on the hanging wall of faults. The epicenter of the 1992 M5.8 St. George earthquake is indicated by the red and white symbol, labeled "EQ" (Christenson, 1995). Approximate areal distribution of the Marysvale volcanic field is outlined by dashed lines. Blue box indicates the location of Red Canyon (RC), where Hecker (1993) constrained slip rate along the Sevier fault. Study area boxed in white. Fold data are from Doelling and Davis (1989), Bowers (1991), and Stewart and Taylor (1996). Digital shaded relief modified from Thelin and Pike (1991). Figure modified from Hecker (1993), Reber et al. (2001), Surpless and McKeighan (2022), and Taylor et al. (2024)..

width of the damage zone and fault displacement are proportional, with width increasing at a constant ratio as displacement accumulates (e.g., Shipton and Cowie, 2001), or if damage zone width occurs rapidly early in a fault's history and increases at a much slower growth rate later in a fault's displacement history (e.g., Savage and Brodsky, 2011; Mayolle et al., 2021, 2023).

In this Keck Utah Advanced Project, three students investigated the evolution of normal fault damage zone development with increasing displacement. Students investigated fault-related fracturing along the central Sevier fault zone in southern Utah (Fig. 2), focusing on damage zone development associated with fault displacements ranging from near zero to nearly 800 meters. Another student studied spectacularly well-exposed normal fault systems in the Tharsis region of Mars to investigate the structural evolution of a segmented normal fault system across a range of scales, and another student performed MATLAB modeling of a normal fault damage zone as a step in determining geothermal energy potential.

BACKGROUND

The Sevier normal fault, considered one of the most important structures in the Basin and Range province (e.g., Davis, 1999; Lund et al., 2008), is part of the Toroweap-Sevier fault system, which extends for more than 300 km from northern Arizona to southern Utah (Fig. 2). The fault has accommodated extension across the transition zone from the Basin and Range province to the relatively stable Colorado Plateau since the Miocene (e.g., Reber et al., 2001; Lund et al., 2008), and previous workers have noted the potential of the fault to produce significant earthquakes (Anderson and Rowley, 1987; Doelling and Davis, 1989; Anderson and Christenson, 1989; Christenson, 1995; Lund et al., 2008). It is likely that many segments of the Sevier fault reactivate older high-angle, Laramide-age contractional structures (e.g., Taylor et al., 2024; Stewart and Taylor, 1996; Schiefelbein and Taylor, 2000), which may explain why the steeply-west-dipping fault zone is segmented in map view, with variations in the geometry of linkages between normal fault segments (e.g., Davis, 1999; Reber et al., 2001; Schiefelbein, 2002; Doelling, 2008).

Three students focused their investigations on a particularly complex portion of the Sevier fault zone, termed the Orderville geometric bend (e.g., Reber et al., 2001; Taylor et al., 2024) (Fig. 3). The Orderville bend displays a range of geometries associated with the interactions of three fault segments, which include the Mt. Carmel segment, the Orderville segment, and the Spencer Bench segment (Taylor et al., 2024). Mapping by Taylor et al. (2024) reveals a network of faults from the latitude of Orderville to the south that display a range of dip-slip displacements (Fig. 3), permitting documentation of changes in damage zone development at different accumulated displacements.

In addition, a fourth student focused their research on the Alba Fossae fault network, which is a circumferential fault system on the west flank of Alba Mons in the northern Tharsis region of Mars, one of the largest volcanoes in the solar system. She addressed research questions about the geometries and variations in displacement, leveraging those data to decipher the initiation and propagation history of the fault system.

Finally, a fifth student used thermodynamic modeling in MATLAB to learn more about how effectively thermal energy transfers from the rock within a damage zone to fluids driven by applied pressure differences. Her research can be applied to utility-scale geothermal plant development, where companies must evaluate the design of injection and withdrawal systems in their assessment of geothermal energy potential.

STUDENT PROJECTS

Three students used the excellent vertical and lateral exposure of the Jurassic Navajo sandstone at the two primary study areas, at Red Hollow Canyon and Elkheart Cliffs (Fig. 3) to directly observe faults and fractures within this well-studied lithology (e.g., Rogers and Engelder, 2004; Schultz et al., 2010; Solom et al., 2010). The Elkheart Cliffs exposure ("3" in Fig. 3) displays the simplest fault geometry because the Mt. Carmel segment accommodates all E-W extension. At the latitude of Red Hollow Canyon (Fig. 3), extensional strain is accommodated by multiple structures, but students focused their research on the southern end of the Spencer Bench segment, where accumulated displacement tapers from ~10 m in the north to the fault tip (0 m), permitting two students to study changes in strain accommodation with changes in displacement (study areas 1 and 2 in Fig. 3).

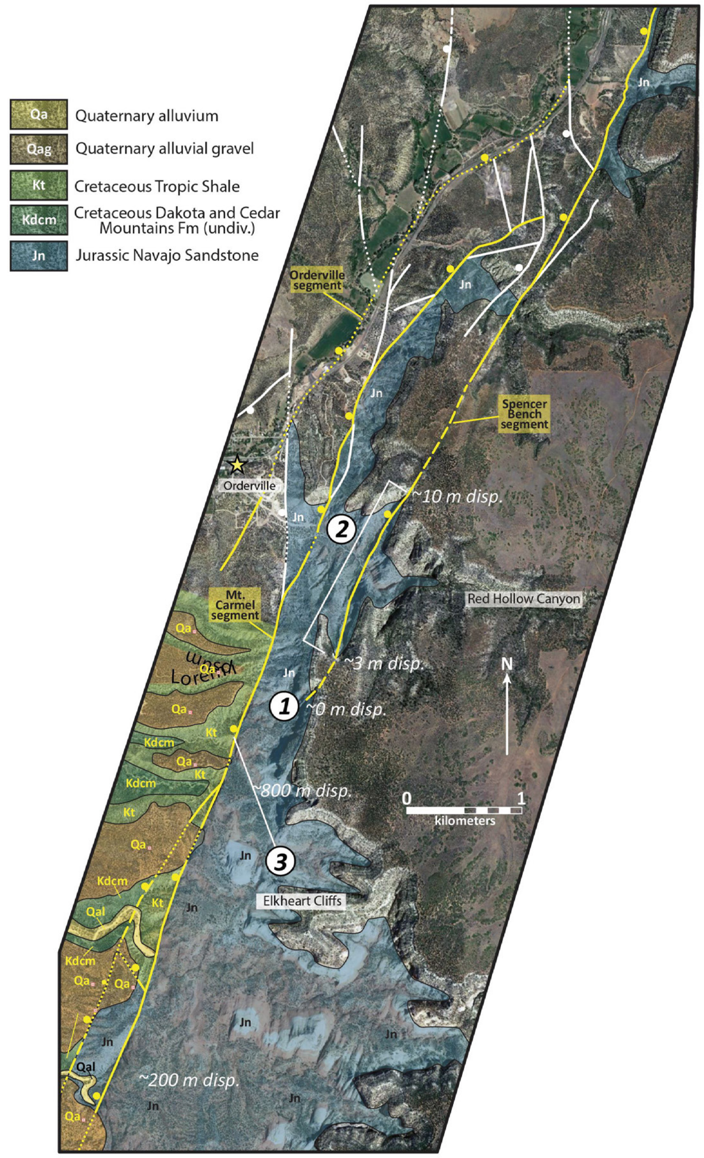

Figure 3. Simplified structural map of the steeply WNW-dipping central Sevier fault zone. Yellow faults represent the primary segments of the fault zone, and the white faults are subsidiary faults that help accommodate extension across the fault network. The blue shaded areas represent exposures of the Jurassic Navajo Sandstone, and areas shaded in transparent greens and yellows are the hanging wall of the Mt. Carmel segment, including: Kt (Cretaceous Tropic Shale), Kdcm (Cretaceous Dakota and Cedar Mountain Formations), Qag (older alluvial gravels), and Qal (modern alluvium). The white circled numbers represent the locations of field and modeling studies performed by Lila Ryter (1), Ariel Montalvo (2), and Sydney Costa (3).

To address fundamental questions about how rock volumes respond to the evolution of complex, segmented, normal fault systems, students applied a variety of approaches, including analysis of field data, 3D digital modeling and analysis of photographic data, MATLAB computer modeling of thermal energy transfer in an enhanced geothermal system, and remote-sensing analysis of a complex, segmented fault system in the Tharsis region of Mars. Their work improves our understanding of the 3D evolution of faults and fracture networks in complex normal fault zones, which has important implications for natural resource exploration.

Sydney Costa (West Chester University) focused her investigation on a locality where the Mt. Carmel segment has accumulated ~800 meters displacement. She used field observations and data in combination with Structure-from-Motion (SfM) model analysis to investigate how fault- damage zones develop in response to high displacements (3 in Fig. 3). Her analysis of the Jurassic Navajo Sandstone revealed a ~100-120m wide footwall damage zone structure consistent with previous studies, with a fault core of concentrated strain as well as an inner and outer damage zone. The fracture network exhibited orientations sub-parallel to the primary fault plane, and the total width of the footwall damage zone is only two to three times the width of the footwall damage zone investigated by Ryter (this volume) despite accumulated displacement that is over 300 times greater, clearly showing that the width of the damage zone envelope around a normal fault system does not increase proportionally with displacement, consistent with Savage and Brodsky (2011). Sydney attributes the change in rate of damage zone width increase to two primary factors in her short contribution.

Demi Durham (Trinity University) used Google Mars to investigate a complex circumferential fault network on the western flank of the Alba Mons volcano in the Tharsis region of northern Mars. She was able to relate map view fault geometries and finite extension estimates to the relationship between topography and the position of volcanic centers to build a new hypothesis for the initiation and evolution of the system.

Demi found that the initiation of the circumferential fault system was likely influenced by both the upward propagation of N-striking dikes and the E-W-oriented local stress field, which was influenced by the uplift and/or subsidence of the volcanic center (e.g., Tanaka, 1990; Ohman and McGovern, 2014). The geometries of the northern and southern portions of the fault system display en echelon geometries that support a fault network influenced by pre-existing faults to the north and south of the volcanic edifice of Alba Mons. The position of the circumferential fault network, with the central system coinciding with the peak of a western volcanic center on the Alba Mons complex, suggests that magmatic overpressure likely added a tensional component that permitted faults to form at that location prior to propagation of the network northward and southward along the western margin of the volcano.

Isabel Garcia (Trinity University) Isabel investigated fluid flow and thermal flux within a simplified enhanced geothermal system (EGS) by modeling the system as a hydraulically fractured cylindrical channel in the subsurface at sufficient depth for high enough temperatures in an extensional setting. The model consisted of nested cylinders with radially decreasing permeability and radially increasing thermal conductivity (rock is more conductive than water). She used Darcy's law to govern fluid flux as a function of distance from the center (r), and she varied the radius and permeability to investigate the effects of these variables on energy flux from the intact rock into the system. She solved the transient heat equation and calculated the thermal flux as a function of r for different cases. She compared this to the fluid flux and extracted the total thermal flux flowing out of the system at the extraction well. This indicates how long the channel would have to be for this simplified system to be a viable source of energy.

Ariel Montalvo (Whitman College) investigated the Spencer Bench fault segment where accumulated displacement tapers southward from ~10 m on the north side of Red Hollow Canyon to ~3 m on the south side of the canyon (Fig. 3). He used field observations and data in combination with Structure-from-Motion (SfM) model analysis to investigate fracture characteristics along the steeply west-dipping fault. He found that hanging-wall fractures were oriented sub-parallel to the fault plane in the best exposures along the segment, and Ariel also learned that fracture intensities were higher in the southern hanging wall, where displacements were lower. This suggests that at least at low displacements, fracture intensities cannot be easily correlated with accumulated displacement.

Ariel also learned that the fracture intensity values in the hanging wall were much higher than in the footwall, consistent with previous studies that suggest asymmetry in normal fault damage zones (e.g., Berg and Skar, 2005; Liao et al., 2020). Finally, Ariel documented that the orientation of steeply dipping fractures in the footwall displayed strikes rotated about 25 degrees clockwise relative to the fault-parallel fractures in the hanging wall. Ariel provides hypotheses to explain these data.

Lila Ryter (Beloit College) used Structure-from-Motion (SfM) model analysis to investigate how fault-damage zones develop (Fig. 1) in response to the very low displacements near the fault tip of the Spencer Bench segment. She learned that fracture intensity in the hanging wall damage zone was higher than in the footwall, and she also learned that the width of the hanging wall damage zone was wider than the footwall damage zone. In addition, Lila found that the footwall damage zone width at very low displacement values (<2.5 m) was approximately 40-m wide, while the width of the nearby Mt. Carmel segment, with displacements of 200 – 800 meters, was just 100-120 m wide. Thus, when combined with Sydney's findings, damage zone widths do not scale linearly with accumulated displacements and support a model of damage zone development with growth early in the displacement history and much slower widening as displacement accumulates. Her findings are consistent with the model presented by Savage and Brodsky (2011).

ACKNOWLEDGEMENTS

This material is based upon work supported by the Keck Geology Consortium and the National Science Foundation under Grant No. 2050697. It was also supported by NSF Award 2042114 to PI Surpless. Finally, funding was provided by the Geosciences Department at Trinity University, including funding from the Roy and Tinker Funds to support undergraduate student research.

REFERENCES

Anderson, R.E., and Christenson, G.E., 1989, Quaternary faults, folds, and selected volcanic features in the Cedar City 1°x2° quadrangle, Utah: Utah Geological and Mineral Survey Miscellaneous Publication 89-6, 29 p.

Anderson, J.J., and Rowley, P.D., 1987, Geologic map of the Panguitch NW quadrangle, Iron and Garfield Counties, Utah: Utah Geological and Mineral Survey Map 103, 8 p. pamphlet, scale 1:24,000.

Berg, S., and T. Skar, 2005, Controls on damage zone asymmetry of a normal fault zone: Outcrop analyses of a segment of the Moab fault, SE Utah: Journal of Structural Geology, 27, 1803–1822, doi: 10.1016/j.jsg.2005.04.012.

Bowers, W.E., 1991, Geologic map of Bryce Canyon National Park and vicinity, southwestern Utah: United States Geological Survey Miscellaneous Investigations Series Map 2180, 1:24,000.

Choi, J-H., Edwards, P., Ko, K., and Kim, Y-S., 2016, Definition and classification of fault damage zones: a review and a new methodological approach: Earth Science Reviews, v. 152, p. 70-87.

Christenson, G.E., ed., 1995, The September 2, 1992 ML 5.8 St. George earthquake, Washington County, Utah: Utah Geological Survey Circular 88, 41 pp.

Davis, G., 1999, Structural geology of the Colorado Plateau region of southern Utah, with special emphasis on deformation bands: Geological Society of America Special Paper 342.

DeWitt, E., Thompson, J., and Smith, R., 1986, Geology and gold deposits of the Oatman district, northwestern Arizona: U.S. Geologic Survey Open-File Report 86-0638, 34 p.

Doelling, H.H., 2008, Geologic map of the Kanab 30'x60' quadrangle, Kane and Washington Counties, Utah, and Coconino and Mohave Counties, Arizona, 1:100,000-scale: Utah Geological Survey, MP-08-2DM.

Doelling, H.H., and Davis, F.D., 1989, The geology of Kane County, Utah, with sections on petroleum and carbon dioxide by Cynthia J. Brandt: Utah Geological and Mineral Survey Bulletin 124, 192 p., scale 1:100,000, 10 plates.

Faulds, J., 1996, Geologic map of the Fire Mountain 7.5' quadrangle, Clark County, Nevada, and Mohave County, Arizona: Nevada Bureau of Mines and Geology Map 106, scale 1:24,000 (with accompanying text).

Ferrill, D., Morris, A., McGinnis, R., Smart, K., and Ward, W., 2011, Fault zone deformation and displacement partitioning in mechanically layered carbonates: The Hidden Valley fault, central Texas: AAPG Bulletin, v. 95, p. 1383-1397.

Fossen, H., 2016, Structural Geology: Cambridge University Press, Cambridge, UK, 510 p.

Hecker, S., 1993, Quaternary tectonics of Utah with emphasis on earthquake-hazard characterization: Utah Geological Survey Bulletin 127, p. 1-31.

Hudson, M., 1992, Paleomagnetic data bearing on the origin of arcuate structures in the French Peak – Massachusetts Mountain area of southern Nevada: Geological Society of America Bulletin, v. 104, p. 581 – 594.

Kim, K.-S., Peacock, D., and Sanderson, D., 2004, Fault damage zones: Journal of Structural Geology, v. 26, p. 503–517.

Liao, Z., Hu, L., Huang, X., Carpenter, B.M., Marfurt, K.J., Vasileva, S., and Zhou, Y., 2020, Characterizing damage zones of normal faults using seismic variance in the Wangxuzhuang oilfield, China: Interpretations v. 8, p. 1- 24.

Long, J., and Imber, J., 2011, Geological controls on fault relay zone scaling: Journal of Structural Geology, v. 33, p. 1790 – 1800.

Lund, W.R., Knudsen, T.R., and Vice, G.S., 2008, Paleoseismic reconnaissance of the Sevier fault, Kane and Garfield Counties, Utah: Utah Geologic Survey Special Study 122, Paleoseismology of Utah, v. 16, 31 p.Lowe, D., 2004, Distinctive image features from scale invariant keypoints: International Journal of Computer Vision, v. 60, p. 91–110, doi: 10 .1023 /B: VISI .0000029664 .99615.94.

Lundstern, J-E., and Zoback, M.D., 2020, Multiscale variations of the crustal stress field throughout North America: Nature Communications, v. 11:1951, https://doi.org/10.1038/s41467-020-15841-5.

Mayolle, S., Soliva, R., Dominguez, S., Wibberley, C., and Caniven, Y., 2021, Nonlinear fault damage zone scaling revealed through analog modeling: Geology, v. 49, p. 968-972, doi.org/10.1130/G48760.1.

Mayolle, S., Soliva, R., Dominguez, S., and Wibberley, C., 2023, Normal fault damage zone growth in map view from analogue models: Journal of Structural Geology, v. 176, 104975, doi: 10.1016/j-jsg.2023.104975

Morley, C., Nelson, R., Patton, T., and Munn, S., 1990, Transfer zones in the East African Rift system and their relevance to hydrocarbon exploration in rifts: American Association of Petroleum Geologists Bulletin, v. 74, p. 1234 – 1253.

Öhman, T., and McGovern, P. J., 2014, Circumferential graben and the structural evolution of Alba Mons, Mars. Icarus, 233, 114–125. https://-doi.org/10.1016/j.icarus.2014.01.043

Peacock, D.C.P., and Sanderson, D.J., 1996, Effects of propagation rate on displacement variations along faults: Journal of Structural Geology, v. 18, p. 311 –320.

Reber, S., Taylor, W., Stewart, M., and Schiefelbein, I., 2001, Linkage and Reactivation along the northern Hurricane and Sevier faults, southwestern Utah, In XXX, Eds., The Geologic Transition, High Plateaus to Great Basin – A Symposium and Field Guide, The Mackin Volume: Utah Geological Association Publication 30, Pacific Section American Association of Petroleum Geologists Publication GB78, p. 379 – 400.

Rogers, C., and Engelder, T., 2004, The feedback between joint-zone development and downward erosion of regularly spaced canyons in the Navajo Sandstone, Zion National Park, Utah: in Cosgrove, J., and Engelder, T., Eds., The Initiaion, Propagation, and Arrest of Joints and Other Fractures: Geological Society of London, Special Publicatin, v. 231, doi: 10.1144/GSL.SP.2004.231

Rowley, P., 1998, Cenozoic transverse zones and igneous belts in the Great Basin, Western United States: Their tectonic and economic implications In Faulds, J.E., and Stewart, J.H., Eds., Accommodation zones and transfer zones: the regional segmentation of the Basin and Range province: Geological Society of America Special Paper No. 343, p. 195-228.

Savage, H.M., and Brodsky, E.E., 2011, Collateral damage: Evolution with displacement of fracture distribution and secondary fault strands in fault damage zones: Journal of geophysical research, v. 116, doi:10.1029/2010jb007665.

Schiefelbein, I., 2002, Fault segmentation, fault linkage, and hazards along the Sevier fault, southwestern Utah [M.S. thesis]: Las Vegas, University of Nevada at Las Vegas, 132 p.

Schiefelbein, I., and Taylor, W., 2000, Fault development in the Utah transition zone and High Plateaus subprovince: Abstracts with Programs, v. 32, No. 7, p. 431.

Schultz, R., Okubo, C., and Fossen, H., 2010, Porosity and Grain Size Controls on Compaction Band Formation in Jurassic Navajo Sandstone: Geophysical Research Letters v. 37, doi: 10.1029/2010GL044909.

Schwartz, D.P., and Coppersmith, K.J., 1984, Fault behavior and characteristic earthquakes – Examples from the Wasatch and San Andreas fault zones: Journal of Geophysical Research, v. 89, p. 5681 – 5698.

Shipton, Z. K., and Cowie, P. A., 2001, Damage zone and slip-surface evolution over mm to km scales in high-porosity Navajo sandstone, Utah: Journal of Structural Geology, v. 23, p. 1825–1844, doi:10.1016/S0191-8141(01)00035-9

Shipton, Z.K., and Cowie, P.A., 2003, A conceptual model for the origin of fault damage zone structures in high-porosity sandstone: Journal of structural geology, v. 25, p. 333–344, doi:10.1016/s0191-8141(02)00037-8.

Siler, D., Hinz, N., and Faulds, J., 2018, Stress concentrations at structural discontinuities in active fault zones in the western United States: Implications or permeability and fluid flow in geothermal fields: Geological Society of America Bulletin, v. 130, No 7, p. 1273 – 1288.

Shervais, J. et al., 2024, Geothermal play fairway analysis, part 1: Example from the Snake River Plain, Idaho, v. 117, p. 1 – 18.

Solum, J., Brandenburg, J., Kostenko, O., Wilkins, S. and Schultz, R., 2010, Characterization of deformation bands associated with normal and reverse stress states in the Navajo Sandstone, Utah: AAPG Bull., v. 94, p. 1453–1475, doi:10.1306/01051009137.

Stewart, M., and Taylor, W., 1996, Structural analysis and fault segment boundary identification along the Hurricane fault in southwestern Utah: Journal of Structural Geology, v. 18, p. 1017 – 1029.

Stock, J., and Hodges, K., 1990, Miocene to recent structural development of an extensional accommodation zone, northeastern Baja California, Mexico: Journal of Structural Geology, v. 12, p. 312 – 328.

Surpless, B.E., and McKeighan, C., 2022, The role of dynamic fracture branching in the evolution of fracture networks: an outcrop study of the Jurassic Navajo Sandstone, southern Utah: Journal of Structural Geology, v. 161. DOI: 10.1016/j.jsg.2022.104664.

Surpless, B., and Thorne, S., 2021, Segmentation of the Wassuk Range normal fault system, Nevada (USA): implications for earthquake rupture and Walker Lane dynamics: Geological Society of America Bulletin, v. 134, p. 39-59, DOI: 10.1130/B35756.1

Tanaka, K.L., 1990, Tectonic History of the Alba Patera-Ceraunius Fossae Region of Mars, in Lunar and Planetary Science Conference Proceedings, Houston, TX, Branch of Astrogeology, US Geological Survey, p. 515–523.

Taylor, W., Surpless, B., and Scheifelbein, I., 2024, Complex fault segment linkage within the Sevier fault zone, southern Utah: Lithosphere, 28 p. doi:10.2113/2024/lithosphere_2023_332.

Tchalenko, J.S., 1970, Similarities between shear zones of different magnitudes: Bulletin of the Geological Society of America, v. 81, p. 1625–1640.

Thelin, G.P., and Pike, R.J., 1991, Landforms of the Conterminous United States - A Digital Shaded-Relief Portrayal: U.S.G.S. Geologic Investigations Series I – 2720